Psychoneuroendocrinology 107 (2019) 148–159

Contents lists available at ScienceDirect

Psychoneuroendocrinology

journal homepage: www.elsevier.com/locate/psyneuen

Activation of the kynurenine pathway and mitochondrial respiration to face allostatic load in a double-hit model of stress

V. Nold[a,b], C. Sweatman[b], A. Karabatsiakis[a], C. Böck[a], T. Bretschneider[c], N. Lawless[d], K. Fundel-Clemens[d], I.-T. Kolassa[a], K.A. Allers[b,*]

[a] Clinical & Biological Psychology, Institute of Psychology and Education, Ulm University, Albert-Einstein-Allee 47, Ulm, Germany
[b] Central Nervous System Disease Research, Boehringer Ingelheim Pharma GmbH & Co. KG, Birkendorferstraße 65, Biberach a. d. Riss, Germany
[c] Drug Discovery Sciences, Boehringer Ingelheim Pharma GmbH & Co. KG, Birkendorferstraße 65, Biberach a. d. Riss, Germany
[d] Target Discovery Research, Boehringer Ingelheim Pharma GmbH & Co KG, Birkendorferstraße 65, Biberach a.d. Riss, Germany

ARTICLE INFO

Keywords:
Chronic stress
Mitochondria
Immune system
Allostasis
Tryptophan catabolism
Plasticity

ABSTRACT

Allostasis is the process by which the body's physiological systems adapt to environmental changes. Chronic stress increases the allostatic load to the body, producing wear and tear that could, over time, become pathological. In this study, young adult male Wistar Kyoto rats were exposed to an unpredictable chronic mild stress (uCMS) protocol to increase allostatic load. First, physiological systems which may be affected by extended uCMS exposure were assessed. Secondly, 5 weeks of uCMS were used to investigate early adaptations in the previously selected systems. Adverse experiences during developmentally sensitive periods like adolescence are known to severely alter the individual stress vulnerability with long-lasting effects. To elucidate how early life adversity impacts stress reactivity in adulthood, an additional group with juvenile single-housing (JSH) prior to uCMS was included in the second cohort. The aim of this work was to assess the impact of chronic stress with or without adversity during adolescence on two domains known to be impacted in numerous stress-related disorders: mitochondrial energy metabolism and the immune system. Both, uCMS and adolescence stress increased kynurenine and kynurenic acid in plasma, suggesting a protective, anti-oxidant response from the kynurenine pathway. Furthermore, uCMS resulted in a down-regulation of immediate early gene expression in the prefrontal cortex and hippocampus, while only rats with the double-hit of adolescent stress and uCMS demonstrated increased mitochondrial activity in the hippocampus. These results suggest that early life adversity may impact on allostatic load by increasing energetic requirements in the brain.

1. Introduction

Several diseases have been found to be associated with chronic stress exposure, such as immune and metabolic dysfunction, and psychiatric or neurological disorders (Bisht et al., 2018; Chen et al., 2018a; Deak et al., 2017; Deschenes et al., 2018; Kraynak et al., 2018; Mellon et al., 2018; Ohno, 2017; Patist et al., 2018; Pearson-Leary et al., 2017; Stefanaki et al., 2018; Wirtz and von Kanel, 2017). It is commonly accepted that certain pathologies (excess oxidative stress, altered immune function, deregulated HPA-axis signaling (Rezin et al., 2008; Bauer, 2008; Maes et al., 2012; Srivastava et al., 2018) are present in such disorders and may be the result of stress history. Presumably there is a pre-pathological state and when a certain threshold is reached, allostatic load pushes these systems beyond adaptation. Our interest is to investigate physiological systems known to be disrupted in patients. The goal is to have translational biomarkers related to depressive symptoms. A secondary goal, in particular with regards to this study, is to be able to assess the mechanisms of adaptation that precede pathology, with an aim to learn how adaptation failure leads to pathology. To this end, young adult male Wistar Kyoto rats, which are thought to be sensitive to stress (Gomez et al., 1996; Redei et al., 2001; Solberg et al., 2001), were subjected to unpredictable chronic mild stress (uCMS). This model is broadly used to induce depressive-like behaviour (Armario et al., 1995; Baum et al., 2006; Will et al., 2003). However, it is difficult to say with certainty whether a behavioral phenotype in rodents truly reflects depressive behaviors in humans. Hence, we aimed to assess physiological processes occurring during adaptation to stress instead of behavior which might provide a better comparison with patients (Rezin et al., 2008).

Glucocorticoid induced immune signals resulting in the synthesis

* Corresponding author.
E-mail address: kelly.allers@boehringer-ingelheim.com (K.A. Allers).

https://doi.org/10.1016/j.psyneuen.2019.04.006
Received 12 December 2018; Received in revised form 27 March 2019; Accepted 5 April 2019

and release of pro-inflammatory cytokines prepare against potential tissue damage and pathogen encounter associated with a stressor, but can also be observed as an end result of long-term stress exposure and allostatic overload (Pearson-Leary et al., 2017; Wirtz and von Kanel, 2017; Bauer, 2008; Maes et al., 2012; Piskunov et al., 2016; Miller et al., 2002; Wright, 2009). Studies in rats have shown that distress induces changes in the amount and distribution of peripheral immune cells (Dhabhar et al., 2012; Swan and Hickman, 2014) and microglia (Tynan et al., 2010). Furthermore, altered bioenergetics during stress responses and inflammation were reported (Buttgereit et al., 2000; Delmastro-Greenwood and Piganelli, 2013; Rupprecht et al., 2012; Assmann and Finlay, 2016; Lopez-Armada et al., 2013; Pearce and Pearce, 2013), which conversely can increase reactive oxygen species (ROS) levels to trigger an immune response (Chen et al., 2018b). These neuro-immune and stress-related cascades provide physiological biomarkers that can be monitored. In this study, classical blood counts were measured to observe the overall circulating immune cell profiles. In addition, tryptophan catabolites (TRYCATs) of the kynurenine pathway were measured in blood and cerebrospinal fluid (CSF) because they recently have been suggested as novel biomarkers for depression (PS216, 2016; Schwarcz, 2016). The differential induction of involved enzymes makes profiling of TRYCATs a promising proxy for an inflammatory state: Stress-induced glucocorticoid release leads to an upregulation of the enzyme TDO, which converts tryptophan to kynurenine, mostly in the liver (Gibney et al., 2014; Ohta et al., 2017; Soichot et al., 2013). However, the IDO enzyme, which also converts tryptophan to kynurenine, is induced by cytokines. In the presence of inflammation, activated microglia and macrophages convert kynurenine further to quinolinic acid (due to upregulation of KMO/KYNU/HAAO enzymes), which is an NMDA-receptor agonist and potential neurotoxin due to its oxidative properties (Pérez-De La Cruz et al., 2012; Campbell et al., 2014; Asp et al., 2011; Smith et al., 2001). In an anti-inflammatory state, the excess kynurenine may be further processed to kynurenic acid, which has anti-oxidant properties and hence is considered protective (Lugo-Huitron et al., 2011). Profiling of the kynurenine pathway therefore provides insights into the inflammatory state of the immune system and the antioxidant defense system. Therefore, in an inflammatory state, quinolinic acid is increased relative to any change that might be present in kynurenic acid (Campbell et al., 2014).

Alterations in blood concentrations of TRYCATs have been detected in patients, possibly giving an indication of inflammatory or stress history (de Punder et al., 2018; Demir et al., 2015). Kynurenine was reported to promote resilience (Notarangelo et al., 2018), while decreased levels of kynurenic acid and increased levels of quinolinic acid were associated with depression (Doolin et al., 2018).

To determine new mechanisms that could help to treat or even prevent disease, tracking adaptations or the induction of pathology in brain, in addition to the peripheral immune system is critical. Our focus is in the regions of the medial prefrontal cortex (PFC) and the hippocampus. Due to its role in planning complex cognition, and moderating social behavior, by orchestrating thoughts and actions in accordance with internal goals, the PFC is a brain region largely responsible for the way how stress is perceived and responded to. Indeed, the PFC is associated with stress vulnerability and resilience, and has been largely implicated in stress-related disorders, particularly depression, post-traumatic stress disorder, and anxiety (Han and Nestler, 2017; Wang et al., 2014; Holmes et al., 2018). Chronic stress paradigms have demonstrated a myriad of changes to the PFC, including volumetric, connectivity, and electrophysiological alterations (Belleau et al., 2018; Popoli et al., 2011; Shepard and Coutellier, 2018; Goldwater et al., 2009). In order to keep its influence on connected brain regions like the hippocampus and amygdala updated to the recent experiences, a high level of plasticity is required in the PFC: by changing its hard-wiring on a synaptic level, the PFC enables adaptation to the current environment and regulates future stress assessment. The hippocampus is strongly involved in the latter since it is the CNS region where memory formation and recall occur. Stress has been associated with both enhanced or diminished memory, which can directly be linked to increased and decreased metabolic requirements in the hippocampus, respectively (Osborne et al., 2015). Our approach to investigating potential adaptive processes in the PFC and the hippocampus was two-fold: First, an extended period of 14 weeks of uCMS was applied in which standard behavioral testing (Forced Swim Test, Open Field Test, Sucrose Preference Test) was included to validate the protocol. *Ex vivo*, next generation sequencing (NGS) of the PFC and hippocampus was performed to assess which physiological systems may be affected by uCMS. Second, a 5 week uCMS exposure was used to determine the early adaptive transcriptional changes in the PFC with a focus on how plasticity may be affected. Since the hippocampus is particularly vulnerable to compromised energy metabolism and chronic stress has been demonstrated to accelerate hippocampal aging via this mechanism (Smith, 1996), hippocampal tissue from this second cohort was examined for effects of stress on bioenergetics using high-resolution respirometry. As adolescence was suggested to be a developmentally sensitive period during which the individual stress vulnerability is shaped (Zannas and Binder, 2014; Tzanoulinou and Sandi, 2017; Gomes et al., 2016; Entringer et al., 2016), a preconditioning of adolescent stress inflicted by 5 weeks of juvenile single-housing (JSH) was included in the second cohort.

Allostasis is the process by which the body's physiological systems adapt to environmental changes (McEwen, 2004). Chronic stress increases the allostatic load to the body, producing wear and tear that could, over time, become pathological. Early life adversity was suggested to accelerate this process, but the understanding how initially adaptive alterations join up into pathology is far from complete. In this study we propose two hypotheses: First, uCMS can be used to model allostasis and potentially allostatic overload. This could be evidenced by alterations in systems relevant in human depression, although not necessarily identical to changes observed in patients if the animals are still adapting to the stress. Second, we hypothesized that the double hit of JSH followed by uCMS during early adulthood could add up to a higher cumulative stress load and that aspects of allostatic stress responses would differ mechanistically between the single and the double stress group. Taken together, our aim is to provide new insights into allostatic mechanisms involved in a 'prodromal' phase of stress-induced pathology.

2. Methods

2.1. In vivo experiments

2.1.1. Animal housing

Test-naïve male Wistar Kyoto rats were obtained from Charles River with a bodyweight of about 100 g and an age of 5 weeks in March (cohort 1) or October (cohort 2). The rats were randomly assigned into the experimental groups and habituated to an inverse 12 h light cycle (lights on at 18:00, lights off at 6:00 with a ramp of 30 min) for 5 weeks. During their time in the specific pathogen free animal care facility at Boehringer Ingelheim Pharma GmbH & Co KG, the animals were housed in groups of three in type III Macrolon-cages (900 cm^2, 15 cm height, stainless steel wire cover) with enrichment or single-housed in type II Macrolon-cages (400 cm^2, 14 cm height, stainless steel wire cover) without enrichment (JSH). Enrichment consisted of a red plastic shelter, a red plastic tube, wood wool and a wooden stick for chewing. During the course of the entire experiment, animals were housed in a temperature- (25.5 ± 0.5 °C) and humidity- (50 ± 5%) controlled environment, while food (AIN-93 G basic diet 2222.PH.A05, Kliba Nafag, Switzerland) and tap water was available ad libitum if not contradicted by the uCMS protocol. Controls were continuously shielded from odors and noises of the stress rats by a Scantainer (Scanbur, Denmark). Aspen shavings were exchanged every Monday

morning by the same care taker, if not earlier as part of the uCMS protocol.

2.1.2. Unpredictable chronic mild stress

From an age of 10 weeks onwards, the uCMS protocol started. Nine formerly group-housed rats (uCMS group); and in cohort 2 additionally 9 JSH rats (JSH + uCMS group); were subjected to the uCMS procedure and single-housed, while 9 controls remained group-housed. Mild stressors used in this protocol involved e.g. wet bedding, frequent changes of the bedding, timely limited food and water restriction, intruder confinements, reduction of provided space and flashing lights and were applied in a scheduled manner using 2 designs to increase unpredictability. A detailed chart of the uCMS procedure can be found in appendix A. The stressors were applied by the same experimentor and the order in which group the stressor was performed first was randomized. In cohort 1, behavioural testing was performed in addition to the stressors of the uCMS protocol, while in cohort 2 no behavioural testing was performed to reduce potential confounding effects of excessive handling.

2.1.3. Sucrose preference test

Following 21 h of food and water deprivation, rats were placed into a cage for 1 h with access to 2 drinking bottles, attached to an automated weighing system (TSE Systems, Labmaster). One bottle contained tap water, the other a 2% sucrose solution. By measuring the weight of the bottles each minute, quantities and patterns of drinking behaviour was identified. During the first 8 sessions, the position of the 2% sucrose solution was alternated, training the rat to actively search for the sucrose solution. From training session 8 onwards the position of the sucrose solution remained constant in order to distinguish between rats that actively search for the sucrose and those displaying a side preference. Training was performed twice weekly on Tuesday and Friday until the rats reached an age of 10 weeks. After 11 training sessions, 18 of 24 trained rats actively sought the sucrose, demonstrated by drinking from both bottles before settling on drinking sucrose. These 18 rats were taken into the study and formed cohort 1.

2.1.4. Forced swim test

Is contrast to the standard Porsolt Forced Swim Test, rats were not trained the day before but were only tested once. Rats were placed into 17 cm diameter cylinders containing 30 cm of 25 °C cold water for 5 min and swimming, struggling and immobility were scored by a separate experimenter blinded to the treatment group. Rats were tested after 10 weeks of stress procedure.

2.1.5. Open field test

Rats were placed into the centre of an 83 cm diameter circular arena brightly illuminated from above the centre circle so as to prevent any areas of shadow. The arena was divided into 8 segments with a centre circle measuring 22 cm in diameter. During a period of 3 min, the time to leave the centre circle, rearing, the number of entries into the centre circle and the number of segments entered were determined. Only when all 4 paws were within one segment were counted as entry. Rats were tested at baseline and in weeks 6 and 10 of the uCMS procedure.

2.1.6. Sacrifice

To test for the effect of juvenile single-housing at an age of 10 weeks, 9 controls and 9 JSH-rats of cohort 2 were sacrificed between 7:00–11:00 in the morning under deep anaesthesia with pentobarbital (intra peritoneal injection of 100 mg/kg body weight, Narcoren®, Boehringer Ingelheim Pharma GmbH & Co KG, Germany). Pentobarbital was selected, because other narcotics were described to influence respirometric performance (Takaki et al., 1997). Since high-resoultion respirometry requires the use of fresh tissue, the final sacrifice of cohort 2 was staggered over Monday - Wednesday with 3 rats of each group being sacrificed per day in alternating order of groups, while cohort 1 was sacrificed on one day. All experiments were conducted under the approval of the Regierungspräsidium Tübingen in accordance with the EU Directive 2010/63/EU for animal experiments.

2.2. Ex vivo analyses

2.2.1. Quantification of fecal corticosterone

Samples of feces were collected directly from the rats at 10 a.m. once weekly. Additional fecal samples were collected at 2 p.m., 10 p.m. and 6 a.m. one day prior to sacrifice. Samples were frozen at −20 °C and dried in a lyophylisator. Dried samples were pestled in a mortar pre-cooled with liquid nitrogen. Ethanolic extracts were obtained from 50 mg of fecal powder of each sample. Samples were resuspended in assay buffer and a competitive enzyme-linked immune assay (Cayman Chemicals, Ann Arbor, Michigan, USA) was performed following the manufacturer's instructions.

2.2.2. Mass-spectrometrical determination of TRYCATs

Quantification of plasma and cortico-spinal-fluid (CSF) levels of tryptophan (TRP) and its catabolites kynurenic acid (KYNA), kynurenine (KYN) and quinolinic acid (QUIN) was performed by liquid chromatography tandem mass spectrometry (HPLC-MS/MS). All analytes were quantified simultaneously in one assay. The assays comprised sample clean-up by protein precipitation with ice-cold methanol followed by reversed phase chromatography and mass spectrometric detection in the positive ion multiple reaction monitoring mode using the deuterated analogues of the analytes, namely d_5-kynurenic acid, d_4-kynurenine, and d_3-quinolinic acid as internal standards. The lower limits of quantification in plasma were 625 nM for TRP, 62.5 nM for KYN; 12.5 nM for KYNA and 25 nM for QUIN. The lower limits of quantification in CSF were 1250 nM for TRP, 1 nM for KYN, 5 nM for KYNA and 25 nM for QUIN.

2.2.3. Blood counting

Under deep pentobarbital anaesthesia, a cardiac puncture was performed to draw a critical volume of blood. An aliquot of 750 µl was used for blood count analyses, which were performed on a Siemens Advia 2120i (Siemens Healthcare GmbH, Erlangen, Germany).

2.2.4. High-resolution respirometry

High-resolution respirometry to assess mitochondrial function can give a detailed view of the activity of the electron transport chain (ETC) and its coupling to ATP production, therefore providing some hints to the energetic requirements of the investigated tissue. The rostral halves of the right hippocampi were isolated and stored in ice-cold custodial® (DR. FRANZ KÖHLER CHEMIE GMBH, Bensheim, Germany) to stabilize the tissue prior to respirometry. For measuring oxygen consumption, tissue was homogenated, diluted to a concentration of 2 mg/ml with mitochondrial respiration medium MiRO5 (Oroboros Instruments, Innsbruck, Austria) and loaded into the calibrated oxygraph chambers which were pre-warmed to 37 °C. Measurements were performed in duplicates. The respirometry was conducted following the recommendations of the manufacturer (Oroboros Instruments, Innsbruck, Austria) using the measurement protocol described in (Pesta and Gnaiger, 2012).In brief, pyruvate (5 mM), glutamate (10 mM) and malate (0.5 mM) as substrates for complex I of the ETC and cytochrome c (10µM) as indicator of mitochondrial membrane integrity were added subsequently. After the supplementation with ADP (5 mM) and the complex III substrate succinate (10 mM), the routine respiration was measured. By injecting oligomycin (2.5µM), ATP-sythase was inhibited and hence induced the LEAK state of respiration during which the oxygen is consumed to compensate for the leakage and slippage of ions and cation cycling across the inner mitochondrial membrane. Next the uncoupler FCCP was titrated in steps of 0.5µM to determine the maximal capacity of the ETC. By afterwards adding rotenone (0.5µM) the amount of oxygen which is consumed due to the activity of complex

II−IV alone was determined. Lastly, antimycin A (2.5μM) as inhibitor of complex III was injected to measure the residual oxygen consumption (ROX) outside of mitochondria. All chemicals were purchased from Sigma-Aldrich (Sigma-Aldrich Company Ltd., St. Louis, Missouri, USA). During the measurement of one control animal, the obtained signal of oxygen concentration was not stable in one measurement chamber, so this measurement was excluded and only the values obtained in the stable chamber were used. Furthermore, we excluded 1 animal from each group, due to a lack of responsiveness after supplementation with substrates, which is an indicator of damaged samples. Lastly, one control animal was excluded, due to an increased dose of pentobarbital needed.

2.2.5. Citrate synthase assay

The activity of citrate synthase in the frozen homogenates of hippocampus was detected photometrically. By coupling the synthesis of citrate and CoA-SH from oxalacetate and acetyl-CoA with the formation of TNB out of DTNB and CoA-SH, the activity of the citrate synthase was measured as the rate of increase in absorbance. In brief, 0.1 M triethanolamine HCl buffer, oxalacetate (10 mM), DTNB (1.01 mM) and the citrate synthase standard were freshly prepared on every experimental day. Distilled water was loaded into 1 ml glass cuvettes together with 100 µl of DTNB, 50 µl oxalacetate, 25 µl acetyl CoA and 25 µl Triton and sample or standard. The absorbance was measured at 32 °C.

2.2.6. Next generation sequencing

2.2.6.1. RNA extraction, Illumina library preparation and sequencing. RNA was extracted from each tissue using the Ambion Magmax™-96 RNA isolation kit (Life Sciences) according to the manufacturer's instructions. Briefly, cells were placed in the lysis solution and homogenized in Qiagen Tissuelyzer™ for a period of 30 s. Nucleic acids were captured onto magnetic beads, washed and treated with DNase. Total RNA was then eluted in 30 µl nuclease free water. RNA integrity and concentration were assessed using the Fragment Analyzer and the Standard Sensitivity RNA kit (DNF-471, Advanced Analytical). High quality RNA samples with RIN > 7 were selected for further processing.

2.2.6.2. mRNA library preparation and sequencing. Fifty nanograms of total RNA were used as input material for the NEBNext Poly(A) mRNA Magnetic Isolation Module and the subsequent NEBNext Ultra™ II Directional RNA Library Prep Kit (New England Biolabs). NEBNext Adaptors for Illumina were diluted 100 fold prior to cDNA ligation. Adaptor ligated cDNA was amplified via 14 PCR cycles using NEBNext unique dual index primers (New England Biolabs). PCR products were cleaned up using AMPure XP Magnetic Beads (Beckman Coulter). mRNA libraries were qualitatively and quantitatively assessed using the 1–6000bp NGS kit (DNF-473, Advanced Analytical) and the Quant-iT PicoGreen dsDNA Assay kit, respectively. Final libraries yields were ˜40 nM, while fragment size were ˜ 350bp. Libraries were normalized, pooled and clustered on the cBot Instrument using the TruSeq SR Cluster Kit v3 (GD-401 − 3001, Illumina Inc, San Diego, CA). The clustered flowcells were sequenced on a HiSeq 3000 using a read length of 84 bases in single-read mode, generating an average of ˜30 million pass-filter reads per sample.

2.2.6.3. RNA-Seq data processing. RNA-Seq reads were aligned to the Rat genome using the STAR Aligner v2.5.2a with their corresponding Ensembl 84 reference genome (http://www.ensembl.org). Sequenced read quality was checked with FastQC v0.11.2 (http://www.bioinformatics.babraham.ac.uk/projects/fastqc/) and alignment quality metrics were calculated using the RNASeQC v1.18. Following read alignment, duplication rates of the RNA-Seq samples were computed with bamUtil v1.u.11 to mark duplicate reads and the dupRadar v1.4 Bioconductor R package for assessment. The gene expression profiles were quantified using Cufflinks software version 2.2.1 to get the Reads Per Kilopbase of transcript per Million mapped reads (RPKM) as well as read counts from the feature counts software package. The matrix of read counts and the design file were imported to R, normalization factors calculated using trimmed mean of M-values (TMM) and subsequently voom-normalized, before subjected to downstream descriptive statistics analysis. Genes with RPKM values > 5 in at least one group were considered in the final analyses to ensure data quality (Sollner et al., 2017). The Benjamini-Hochberg's method was used to correct for multiple testing, and only protein-coding genes with adjusted p value < 0.05, independent of magnitude of change, were considered as differentially expressed and used in the subsequent analyses. To conduct pathway analyses, the PFC and hippocampal gene lists from cohort 1 were imported into Ingenuity.

2.3. Statistical analyses

Earlier uCMS studies performed in-house or external showed sufficient discriminatory power with a sample size of 9 (Demirtas et al., 2014; Sahin et al., 2017; Foyet et al., 2017; Mo et al., 2014) for physiological parameters. This is supported by literature indicating physiological parameters are likely to be less variable than behavioural parameters (Becker et al., 2016) All data of the comparison juvenile single housing vs. control was assessed for departures from normality using the Shapiro Wilk test and heteroscedasticity using Bartlett's or Levene's test where appropriate. Parametric statistical testing was performed for the TRYCAT data with a correction for unequal variances (Welch's *t*-test) while non-parametric Mann-Whitney-U-tests were performed for the blood counts, body weight and adrenal weight. For the comparisons after the uCMS procedure, linear models were compared using one-way analyses of variance (ANOVA). Where required, the ranks were analyzed. The corticosterone data was analyzed with a repeated measurement ANOVA of a mixed linear effect model. Individual measures for different analyses are listed in the associated tables and graphs. No correction for multiple testing was performed, due to the exploratory nature of the study and the high inter-correlation of TRYCAT and respirometric data. All analyses were conducted using R 3.2.4 and tests were considered statistically significant when the *p*-value was smaller or equal to the selected alpha level of 5%.

3. Results

3.1. Behavioural validation of the uCMS protocol

In the first cohort, there were no significant changes to body weight gain, sucrose preference, or sucrose consumption. Significant influence of uCMS was observed in the forced swim test and in open field test (appendix D). In addition, alterations were observed in plasma tryptophan catabolites (appendix D). Next generation sequencing revealed 882 significantly deregulated genes in the PFC, and 431 in the hippocampus. Sixty-two of the de-regulated genes in the PFC reached at minimum a 2-fold-change, while none of the genes in the hippocampus reached this level of deregulation. Ingenuity pathway analysis was used to assess the commonalities in deregulated gene sets (appendix E). The overlap between molecular and cellular functions and physiological systems underlying behavior in hippocampus and PFC is of particular note. The immediate early gene Arc is a component of the behavioural function networks, and its deregulation is correlated between the PFC and hippocampus (appendix D).

3.2. Effect of juvenile single housing

In the second cohort, the effect of JSH alone was assessed prior to subjecting rats to uCMS. In a subset, the diurnal HPA-axis activity was traced and 9 rats of each group were sacrificed for analyses at an age of 10 weeks. No significant differences were determined in body or adrenal weight between groups. There were no significant differences

Table 1
Blood Counts and TRYCAT in CSF After 5 Weeks of Juvenile Single Housing.

	Control (n = 8)			JSH (n = 6)				
	min	median ± IQR	max	min	median ± IQR	max	*U*	*p*
White Blood Cells	0.66	1.9 ± 1.5	4.51	1.34	1.56 ± 0.36	3.21	24	1
Monocytes	0.02	0.05 ± 0.05	0.09	0.03	0.05 ± 0.01	0.14	22	0.8
Lymphocytes	0.48	1.2 ± 1.4	3.88	0.93	1.1 ± 0.3	2.58	24	1
Eosinophils	0.01	0.03 ± 0.01	0.04	0.01	0.02 ± 0.02	0.04	31	0.4
Basophils	0	0.01 ± 0.02	0.08	0	0 ± 0.008	0.01	37	0.08
Neutrophils	0.12	0.41 ± 0.12	0.54	0.31	0.38 ± 0.10	0.55	27	0.7
Platelets	183	582 ± 137	648	536	634 ± 44.8	657	14	0.2
Hematocrit	13.3	43.8 ± 9.4	63.5	43	46 ± 3.3	47.7	22	0.9
Red Blood Cells	7100	8310 ± 293	10050	8010	8345 ± 340	8610	25	1.0
Hemoglobin	12.1	14.5 ± 0.93	18.1	13.7	14.3 ± 0.3	14.6	31	0.4
Mean Peroxidase Index	2.3	9.7 ± 18.1	33.2	2.5	4.2 ± 1.7	8.2	31	0.4
Procalcitonin	0.14	0.45 ± 0.16	0.75	0.37	0.39 ± 0.02	0.42	35	0.2

	Control (n = 8)			JSH (n = 8)				
CSF	min	mean ± sd	max	min	mean ± sd	max	*t*	*p*
TRP	1880	2211 ± 299	2740	2020	2456 ± 343	3020	t(13.7) = -1.5	0.2
KYN	11.9	20.5 ± 8.2	35.2	17.6	27.1 ± 6.3	34.6	t(13.2) = -1.8	0.1
QUIN	50.9	58.6 ± 5.8	70	42.8	60.8 ± 14.3	80.5	t(9.2) = -0.4	0.7
KYN / TRP	0.005	0.009 ± 0.004	0.0155	0.0081	0.011 ± 0.002	0.015	t(11.1) = -1.1	0.3

Unit: Blood counts [1000 cells /µl], hemoglobin [g/dl], hematocrit [%], procalcitonin[%], TRYCAT [nM].

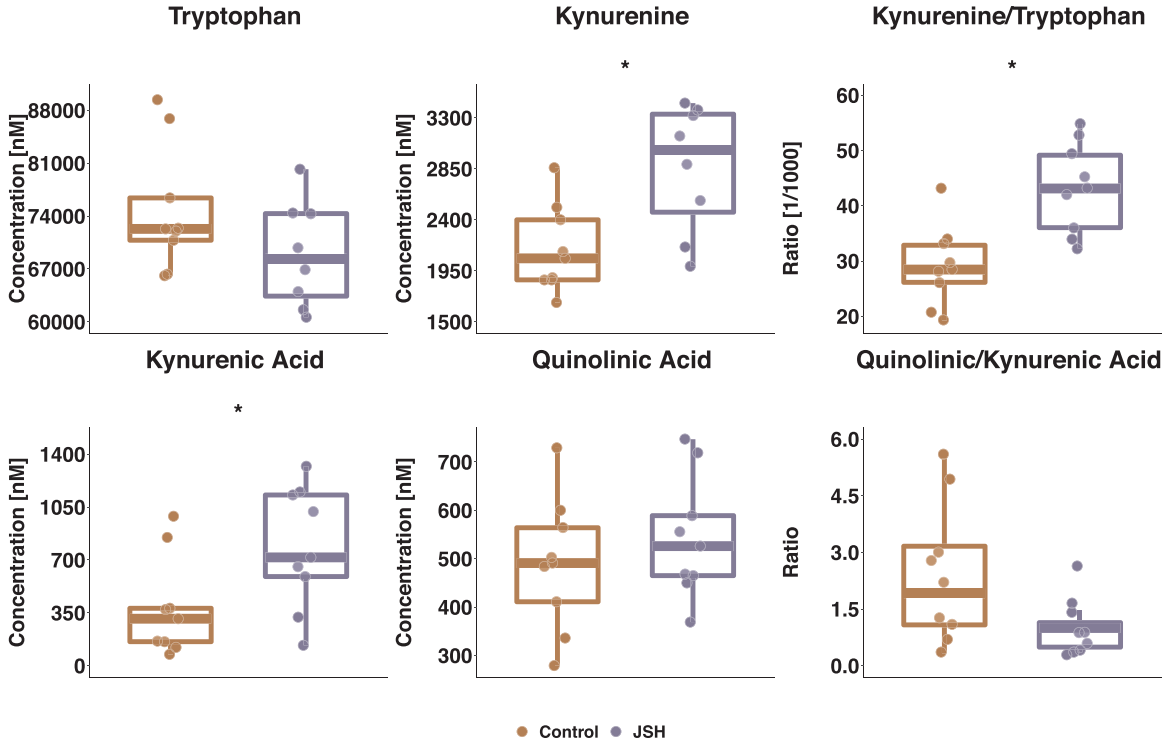

Fig. 1. TRYCAT Profiling After 5 Weeks of Juvenile Single Housing. Plasma concentrations of tryptophan and its catabolites kynurenine, kynurenic acid and quinolinic acid were measured by HPLC-MS/MS. An independent samples *t*-test was conducted to compare plasma levels in 10 weeks old male Wistar Kyoto rats after 5 weeks of single housing during adolescence (violet) and age-matched controls (orange). Results were as follows: tryptophan: t(16) = 1.9, p = .08; kynurenine: t(16) = -3.5, p = .003; kynurenic acid: t(16) = -2.3, p = .03; quinolinic acid: t(16) = -0.9, p = .4; kynurenine/tryptophan: t(16) = -3.9, p = .001; quinolinic acid /kynurenic acid: t(11) = 2.1, p = .06 * = p < .05 in independent samples *t*-test. (For interpretation of the references to colour in this figure legend, the reader is referred to the web version of this article).

in fecal corticosterone at 6 a.m., 10 a.m., 2 p.m. and 10 p.m. between controls housed in groups of three and the JSH group (appendix B). Blood counts and the TRYCATs assessed in CSF did not reveal statistically significant changes attributable to group- vs. single-housing (Table 1). The results of TRYCAT assessment in plasma suggest an effect of the housing condition and are provided in Fig. 1.

3.3. Allostatic load of short-term uCMS exposure

To investigate allostatic processes, rats of the second cohort were subjected to 5 weeks of uCMS with or without JSH as preconditioning to trigger adaptive changed in stress relevant systems.

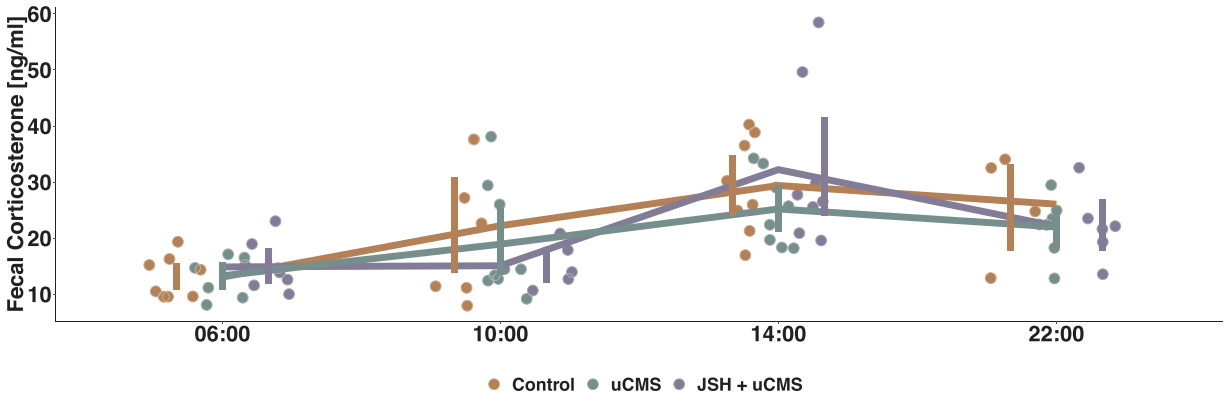

Fig. 2. Diurnal Corticosterone Profile After 5 Weeks of uCMS. At 6:00, 10:00, 14:00 and 22:00, fecal corticosterone levels were measured in rats exposed to five weeks of uCMS (green), rats exposed to 5 weeks of juvenile single housing followed by five weeks of uCMS (violet) and controls (orange). No significant effect of group or the interaction of group and daytime was found. Time showed a significant difference between levels: 6:00 - 14:00 t(54) = -6.4, p < 0.0001; 6:00 - 22:00 t (54) = -3.6, p = 0.003; 10:00 - 14:00 t(54) = -4.0, p = 0.001. Individual data points are shown alongside with the mean ± 95% confidence interval. Repeated measurement two-way ANOVA (group + time | ID), main effect of time: F(3, 48) = 14.4, p < 0.0001 (For interpretation of the references to colour in this figure legend, the reader is referred to the web version of this article).

3.3.1. Diurnal HPA-Axis rhythmicity

The diurnal rhythm of corticosterone excretion in feces was traced after 5 weeks of uCMS exposure (Fig. 2). No statistically significant differences between groups were observed in the overall corticosterone levels as well as at different times of day. A circadian rhythm was present in all groups with a peak at 2 p.m. and a nadir at 6 a.m. in fecal corticosterone concentration.

3.3.2. Kynurenine pathway profiling

After 5 weeks of uCMS, the concentration of quinolinic acid in plasma was decreased in the uCMS group ($t(24) = 4.5, p = .0005$) and in the uCMS rats with additional juvenile single-housing ($t(24) = 4.8$, $p = .0002$) compared to controls. The other TRYCAT measures and ratios were not significantly changed in plasma. In CSF, an increase in the ratio of kynurenine and tryptophan was found which in the post hoc test is significant in the double-hit group ($t(24) = -3, p = .02$). A summary of all TRYCAT [nM] and their ratios is provided in Table 2.

3.3.3. Mitochondrial respirometry

After 5 weeks of uCMS, the activity of the mitochondrial enzyme citrate synthase was significantly affected by group ($F(2,24) = 5.71$, $p = 0.009$). Tukey HSD post-hoc testing revealed an increase in the uCMS group ($t(24) = -2.7, p = 0.03$) and in the group with combined juvenile single-housing combined with uCMS ($t(24) = -3.1, p = 0.01$). The residual oxygen consumption (ROX), which is *per definitionem* independent of mitochondrial respiration, was not different in uCMS rats compared to controls, but the amount of oxygen consumed at routine and LEAK as well as the respiration after uncoupling the ETC and after inhibiting complex I was increased after uCMS, while this increase was more pronounced in the group which additionally had experienced juvenile single housing. Since the amount of oxygen consumption is directly linked to the amount of mitochondria, we normalized the respirometric measurements to the citrate synthase activity, since this is a commonly used surrogate for mitochondrial density. The results of ROX, citrate synthase activity and the normalized high-resolution respirometry are visualized in Fig. 3. After accounting for mitochondrial density, the respiration at routine and without ETC I was still significantly increased in the double-hit group. Notably, the routine flux control, coupling control, coupling efficiency and net-routine were unaltered by stress exposure (data not shown).

3.3.4. Next generation sequencing

A significant decrease in the immediate-early genes *Arc*, *Fos*, *Fosb* and *Npas4* was detected in the PFC of rats which underwent uCMS alone or in combination of juvenile single-housing, compared to controls (Fig. 4).

3.3.5. Blood counts

Rank ANOVA of blood counts suggests that after 5 weeks of uCMS there is an increase in several white blood cells in the stress groups compared to controls. Counts for lymphocytes were increased in both, the uCMS group ($t(22) = -4.5, p = .0005$) and the uCMS group with additional juvenile single-housing experience ($t(22) = -2.8, p = .03$). Eosinophil granulocytes were as well increased in both, the uCMS group

Table 2
TRYCAT Levels and Ratios After 6 Weeks of uCMS.

	Control (n = 9)			uCMS (n = 9)			JSH + uCMS (n = 9)				
CSF	min	mean ± sd	max	min	mean ± sd	max	min	mean ± sd	max	*F (224)*	*p*
TRP	2240	2436 ± 180	2780	1980	2441 ± 382	3340	2120	2284 ± 218	2790	1.0	0.4
KYN	7.4	13.1 ± 4.7	21.5	11.1	18.8 ± 4.5	25	8.4	19.1 ± 7.4	30.8	3.1	0.06
QUIN	42.2	55.4 ± 10.0	70.5	41.2	53 ± 8.1	66.5	48.1	53.2 ± 4.7	63.3	0.3	0.8
KYN / TRP	0.003	0.005 ± 0.002	0.008	0.006	0.008 ± 0.001	0.009	0.004	0.008 ± 0.003	0.013	4.9	0.02*
Plasma											
TRP	58000	68077 ± 9041	83900	51700	65466 ± 11143	83700	49000	60133 ± 7211	69500	1.7	0.2
KYN	989	1773 ± 484	2420	1320	2154 ± 520	2970	1100	2029 ± 635	3050	1.1	0.3
KYNA	224	449 ± 162	720	46.1	510 ± 331	1210	140	489 ± 173	772	0.2	0.9
QUIN	365	476 ± 68.8	543	170	308 ± 94.7	508	166	294 ± 73.7	438	14.0	< .001*
KYN / TRP	0.01	0.027 ± 0.01	0.041	0.02	0.03 ± 0.01	0.05	0.02	0.03 ± 0.01	0.05	1.4	0.3
QUIN / KYNA	0.73	1.152 ± 0.33	1.7	0.25	1.0 ± 1.0	3.7	0.35	0.71 ± 0.42	1.8	1.0	0.4

Unit: Individual TRYCAT measures in nM.

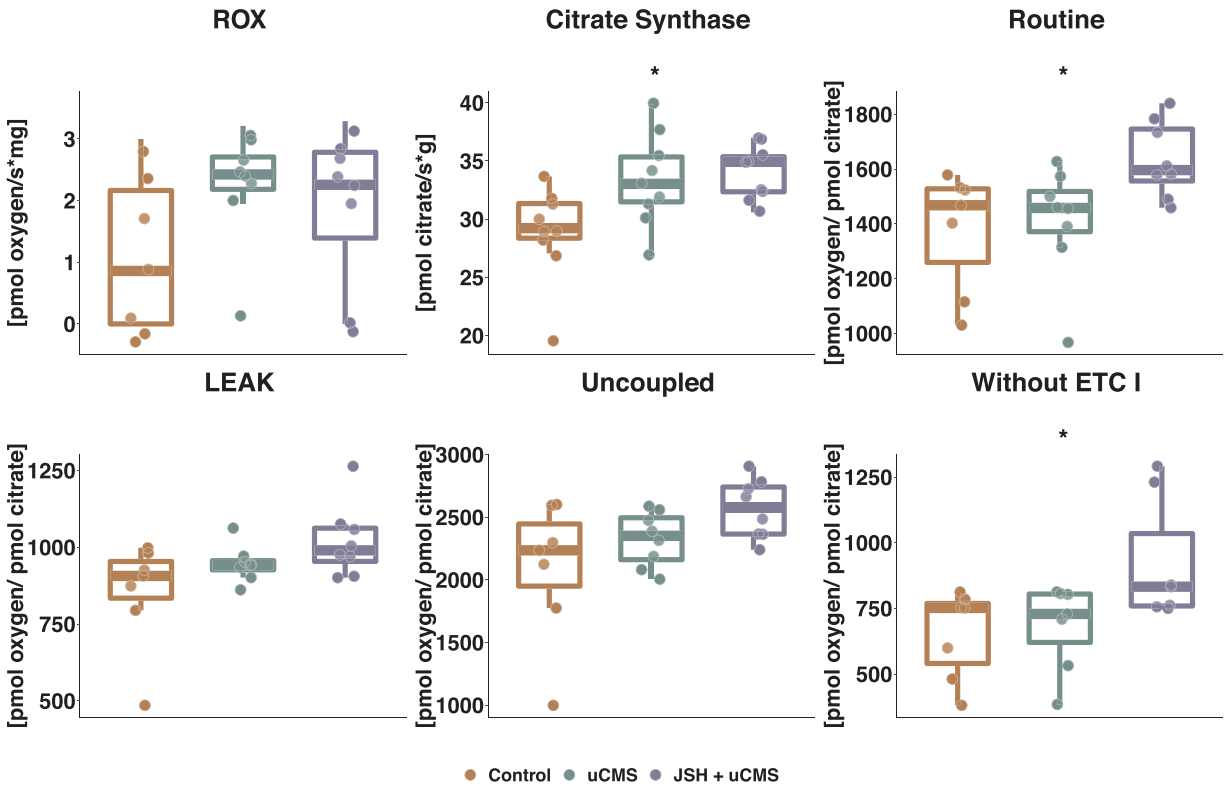

Fig. 3. Respirometry After 5 Weeks of uCMS. Hippocampal respirometric performance was determined in 16 weeks old rats which underwent 5 weeks of juvenile single housing followed by 5 weeks of uCMS (violet), 5 weeks of uCMS (green) and controls (orange). Residual oxygen consumption (ROX) was subtracted from all respirometric measurements to only report oxygen consumption associated with mitochondrial respiration. To account for overall mitochondrial increase, the oxygen consumption was divided by citrate synthase activity. Tukey honest significant difference post-hoc testing suggests an increased routine respiration in the combination of juvenile single-housing with uCMS compared to both, uCMS (p = .0301) and controls (p = .0242). Post hoc testing for respiration without ETC I suggests a borderline increase in juvenile single housed rats with uCMS compared to controls (p = .0529). 1-way-rank-ANOVA (group): Citrate Synthase $F(2,24) = 7$, p = .0042; Routine $F(2,20) = 5.39$, p = .0134;, Without ETC I $F(2,18) = 3.69$, p = .0453 (For interpretation of the references to colour in this figure legend, the reader is referred to the web version of this article).

($t(22) = -4.1$, $p = .001$) and the JSH + uCMS group ($t(22) = -4.9$, $p = .0002$) and basophil granulocytes also showed an increase in the uCMS group ($t(22) = -2.8$, p(uCMS) = .03) and the double-hit group ($t(22) = -5.1$, $p = .0001$). Neutrophil granulocytes were only increased in the double-hit group ($t(22) = -2.6$, $p = .05$). Monocytes were increased in the uCMS group ($t(22) = -5.3$, $p = .0001$) and the juvenile single-housed uCMS group ($t(22) = -5.7$, $p < .0001$). An overview of the findings in blood counts is provided in Table 3.

4. Discussion

In this study, an extensive period of uCMS was used in a first cohort to demonstrate moderate behavioural changes and to explore which physiological systems might play a role in adaptation to uCMS. This

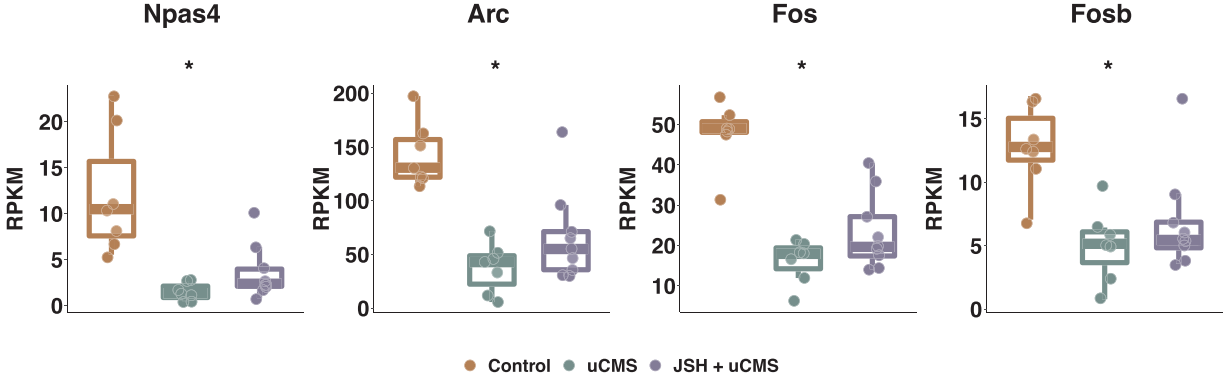

Fig. 4. PFC Gene Expression Profile After 5 Weeks of uCMS. Next-generation sequencing of the PFC was used to compare the uCMS-only group (green) and the double-hit group with juvenile single-housing prior to uCMS (violet) to controls (orange). From all significantly different genes, only the most reliable with RPKM > 5 in at least one experimental group were eligible. There was a statistically significant reduction in the expression of Npas4, Arc, Fos and Fosb in the uCMS groups compared to controls. Results of the post hoc tests in the uCMS-only group were: Npas4 (t(11) = -3.1, p = .006), Arc (t(11) = -1.7, p = .01), Fos (t(11) = -1.5, p = .002) and Fosb (t(11) = -1.2, p = .003). In the double-hit group results were as follows: Npas4 (t(12) = -2.1, p = .02), Arc (t(12) = -1.3, p = .05), Fos (t(12) = -1.2, p = .003) and Fosb (t(12) = -1.2, p = .0004). * = p < .05 in pairwise comparison of control vs. uCMS and control vs. JSH + uCMS (For interpretation of the references to colour in this figure legend, the reader is referred to the web version of this article).

Table 3
Blood Counts After 6 Weeks of uCMS.

	Control (n = 9)			uCMS (n = 8)			JSH + uCMS (n = 8)				
	min	mean ± sd	max	min	mean ± sd	max	min	mean ± sd	max	F(222)	p
White Blood Cells	0.74	1.09 ± 0.24	1.53	1.1	1.6 ± 0.5	2.7	1.01	1.6 ± 0.9	3.8	4.95	0.02*
Monocytes	0.02	0.03 ± 0.01	0.04	0.04	0.06 ± 0.04	0.17	0.03	0.07 ± 0.05	0.19	21.28	< .0001*
Lymphocytes	0.47	0.70 ± 0.14	0.84	0.77	1.1 ± 0.4	2.2	0.61	1.1 ± 0.7	2.9	10.49	0.0006*
Eosinophils	0.01	0.02 ± 0.01	0.03	0.02	0.04 ± 0.02	0.07	0.02	0.4 ± 1.1	3	13.96	0.0001*
Basophils	0	0.003 ± 0.005	0.01	0	0.006 ± 0.005	0.01	0	0.008 ± 0.005	0.01	12.92	0.0002*
Neutrophils	0.21	0.32 ± 0.12	0.62	0.2	4.5 ± 12.0	34	0.31	0.4 ± 0.1	0.6	3.48	0.05*
Platelets	389	503 ± 52.7	565	477	549 ± 75.6	695	410	502 ± 55.4	593	0.69	0.5
Hematocrit	39.6	41.9 ± 1.7	44.3	38.8	42.0 ± 2.5	45.5	39.4	43.0 ± 3.0	48.4	0.24	0.8
Red blood cells	7570	8096 ± 398	8750	7300	7922 ± 423	8640	7380	8086 ± 403	8770	0.43	0.7
Hemoglobin	12	13.1 ± 0.6	14	11.8	13.0 ± 0.7	14.1	12	13.3 ± 0.6	14.3	0.82	0.5
MPXI	4.4	9.1 ± 2.6	12.7	3.8	7.0 ± 2.6	10.9	4.4	7.5 ± 3.2	13.1	1.22	0.3
Procalcitonin	0.31	0.36 ± 0.04	0.4	0.32	0.4 ± 0.05	0.48	0.31	0.4 ± 0.06	0.5	1.01	0.4

Unit: Blood counts [1000 cells /µl], hemoglobin [g/dl], hematocrit [%], procalcitonin[%]; MPXI = mean peroxidase index.

first cohort provided evidence for changes in the kynurenine pathway which was followed up in a second cohort. Furthermore, NGS suggested neuronal activity changes due to reduced expression of the immediate early genes Arc and Fos. This deregulation was correlated between hippocampus and PFC, but was greater in PFC, which led to a focus on the transcriptome from the PFC in the second cohort and the decision to assess cellular health functionally in the hippocampus by using high-resolution respirometry. Respirometry was chosen because decreased mitochondrial functioning or evidence of slowed metabolism which was suggestive in the mild transcriptome changes from cohort 1 has also been observed in depressive patients (Maes et al., 2012; Boeck et al., 2018; De et al., 2017).

In the blood of rats which underwent uCMS for 5 weeks, we saw an increase in the amount of white blood cell populations. In line with earlier publications (Dhabhar et al., 2012), a mobilization of monocytes was present in blood of uCMS-exposed rats. As precursors of macrophages, monocytes are involved in the initiation and propagation of immune reactions and hence could be an early marker for the establishment of a pro-inflammatory milieu (Wang et al., 2015; Stotz et al., 2015; Eo et al., 2016). In our study, increased monocytes levels after stress were accompanied by elevated numbers of granulocytes and lymphocytes. This suggests alterations in the composition of the innate and adaptive immune system following stress. In line with the neuroinflammation hypothesis of depression, increased amounts of immune cells could lead to an increased secretion of pro-inflammatory signaling molecules which in turn could impact the CNS (Kitaoka and Furuyashiki, 2014; Nikolaienko et al., 2018). However, the levels of quinolinic acid were not increased, which would be the case in the presence of increased circulating cytokines. In contrast, quinolinic acid was decreased, which suggests that the activity of immune competent cells was not increased to a biologically relevant point. Nevertheless, TRYCAT profiling revealed that after 5 weeks of single-housing during adolescence, an increased catabolism of the essential amino acid tryptophan was detectable in plasma, which led to an increase in kynurenic acid and its precursor kynurenine. These metabolites are considered to be neuroprotective (Sas et al., 2007), because kynurenic acid inhibits glutamatergic NMDA-receptors and reduces the release of dopamine and glutamate (Capuron and Miller, 2011). Hence, an activation of this side of the kynurenine pathway holds the potential to decrease the excitatory signaling in the brain. Even though tryptophan catabolism was increased in the periphery, which presumably stems from activity of the liver enzyme TDO, kynurenine can exert activity in the CNS, because it can be transported by the large neutral amino acid carrier of the blood brain barrier (Fukui et al., 1991). In the absence of inflammatory processes, kynurenine is converted to kynurenic acid by the astrocytic kynurenine-amino-transferases. The correlation of kynurenine in plasma with its levels in CSF as well as the correlation with its catabolite kynurenic acid in plasma supports this (appendix C). Taken together, blood counts and TRYCAT profiling did not point towards inflammatory processes, but suggested an activation of the neuroprotective and anti-oxidant side of the kynurenine pathway.

The increased amount of NMDA-receptor inhibiting kynurenine and kynurenic acid and reduced NMDA-receptor stimulating quinolinic acid, is suggestive of reduced excitatory neurotransmission. One hypothesis is that this could be reflected as reduced synaptic plasticity (Mattson, 2008; De Pitta and Brunel, 2016; Rebola et al., 2010; Hunt and Castillo, 2012; Jay, 2003; Otani et al., 2003). Our NGS finding that the expression of immediate early genes was reduced in the PFC is supportive of this hypothesis. After 5 weeks of uCMS, immediate early genes like Arc, Fos, Fosb and Npas4 were switched off or significantly reduced in both stress groups compared to controls. Decreased levels of these genes suggest a decreased ability of the PFC to respond to incoming signals by changing its synaptic outputs (Takahashi and Miczek, 2014; Minatohara et al., 2015). Interestingly, synaptic weakening in the PFC has been associated with resilience to stress (Wang et al., 2014). This observation would fit with our interpretation the rats in this study were still coping and undergoing allostasis. An alternative hypothesis could be raised, that reduced plasticity in the PFC might increase the likelihood of insufficient provisions for future challenges, which could render the body more prone to accumulate damage. From a circuit perspective, this could be relevant for the interactions of the PFC and hippocampus under healthy conditions, the hippocampus receives dampening signals from the PFC (Anderson et al., 2016; Godsil et al., 2013). If the hippocampal activity is increased and the plasticity of the PFC is reduced, inhibitory outputs from the PFC may be insufficient, leading to excess hippocampal activity. Excess hippocampal activity could result in the mild transcriptome signature from the first cohort indicating changes to cellular health, and might also be detectable as increased energy consumption.

Indeed, after 5 weeks of uCMS an increased activity of the mitochondrial enzyme citrate synthase was found in hippocampus. This enzyme is a common proxy for the cellular density of mitochondria (Larsen et al., 2012). Since the main energy currency of the body, adenosine-tri-phosphate (ATP), is produced in mitochondria, an increase in their number as measured by citrate synthase, suggests increased energy consumption and hence activity in the rat hippocampus after uCMS. Increased hippocampal activity is directly linked to enhanced memory formation and recall, which has been associated with stress (Osborne et al., 2015). In the pathologic state, such an over-encoding of memory presents as rumination of adverse thoughts in depression and strengthening of the fear-network in post-traumatic stress disorder. Additionally to the increased number of mitochondria, the activity of the ETC was found to be altered in rats exposed to uCMS. However, after normalizing the oxygen consumption to the citrate

synthase activity, only an increased routine respiration and oxygen consumption without ETC complex I in rats which underwent the double stress of JSH followed by uCMS was observed. In turn, this steady energy consumption in the hippocampus might require reallocation of resources, which could be at expense of the PFC. Reduced availability of resources in combination with decreased expression of immediate early genes would render the PFC even less able to inhibit hippocampal activity and a vicious circle is formed, that could over time cumulate in allostatic overload and functional consequences.

If the suggested energetic linkage hypothesis between hippocampus and PFC holds true, our observation that ETC activity was increased only in the double stress group might indicate that these animals are already in the transition from adaptation to pathology. After a certain type or duration of stress, their mitochondria might decompensate due to a mitochondria inherent susceptibility to ROS (Indo et al., 2007; Yakes and Van Houten, 1997; Jendrach et al., 2008) and hippocampal cells could suffer from insufficient energy supply. In our previous uCMS study with triple the duration of uCMS exposure (15 weeks), NGS analyses of hippocampus and PFC both revealed a reduction of immediate early genes (appendix D). This could be a way to adjust energetic demands in order to survive, but is on a slippery slope because it does not solve the original problem. On the long run, even this adjustment might not be enough to rescue hippocampal activity. In depressive patients, reduced mitochondrial respiration as sign for decompensation (Karabatsiakis et al., 2014) and an atrophy of the hippocampus (Opel et al., 2014; Sheline et al., 1996) have indeed been described. Interestingly, a reduction in hippocampal volume in depressive patients has been shown to correlate with TRYCAT profiles, suggesting that perhaps the tipping point revolves around the balance of multiple measures.

Taken together, the alterations observed by respirometry point towards higher energetic demands of the hippocampus after a certain dose or duration of stress. An elevated respiration after inhibition of ETC I with rotenone in the double-hit group compared to controls is indicative for an increased utilization of ETC complex II to fuel ATP production. ETC II serves as alternative entry point for hydrogen abstracted from Flavin-adenin-dinucleotide-dihydrogen while at ETC I NADH is utilized. Interestingly, complex I activity is associated with more production of reactive oxygen species (ROS) than complex II (Liu et al., 2002), so a shift towards complex II might be a possibility to reduce ROS overload and to evade the risk of oxidative stress which is inseparably linked to increased mitochondrial activity. Our observation of decreased quinolinic acid levels at the same time point when mitochondrial changes are present and the moderate negative correlation of quinolinic acid and citrate synthase activity (appendix C) strengthens this idea, because quinolinic acid is a precursor for the ETC I substrate NAD. Whether a reduced availability of quinolinic acid and hence NAD leads to the alternative usage of ETC complex II or whether a mitochondrial mechanism to avoid excessive ROS reduces the quinolinic acid side of the kynurenine pathway is an exciting question for future studies. Either way, the 5 weeks of uCMS, even when combined with juvenile single-housing stress has not induced mitochondrial pathology, since the respirometric control ratios remained unaltered. There was no difference in the relation between oxygen consumption used for ATP production at routine compared to ETC activity solely accounting for leakage of electrons and cation slippage in the LEAK stage. Furthermore, the coupling efficiency of controls and uCMS animals did not differ after 5 weeks of exposure, suggesting that no damage or functional disintegration of the mitochondria had occurred yet. In sum, the alterations in mitochondrial activity observed in this study indicate a healthy coping mechanism, in line with the concept of allostasis being an adaptive process.

In context with our findings from profiling immune cells, TRYCATs and gene expression in the PFC, our mitochondrial data supports the hypothesis that uCMS can be used to model allostasis and potentially allostatic overload. By including juvenile single-housing as preconditioning and using a short-term exposure to uCMS, we extended the uCMS model to better elucidate the initial alterations in physiology as part of an allostatic response and how early life adversity moderates this process. As hypothesized, the double hit of JSH followed by uCMS during early adulthood seemed to add up to a higher cumulative stress load leading to mechanistically different allostatic stress responses in some aspects, since ETC functioning was only altered in the double stress group. Overall, the physiological alterations observed in these studies could be interpreted as origin of allostatic overload. With allostasis being an “active” process, first mitochondrial activity could increase proportional to the amount of adaptation necessary, but later might decompensate due to the inherent vulnerability of mitochondria to ROS (Indo et al., 2007; Yakes and Van Houten, 1997; Jendrach et al., 2008). While decreased mitochondrial functioning has been detected in blood of depressive patients, it is possible that such changes in metabolic processes will be observed in the central nervous system as well. Given the sensitivity of the hippocampus to compromised energy metabolism (Karabatsiakis et al., 2014; Smith, 1996), this brain region is a good starting point to test for this hypothesized link between peripheral and central energy metabolism. The findings in our second cohort of rats support this energetic linking hypothesis. Using a unique combination of innovative readouts in addition to classical readouts used in the clinics, we have discovered that a functional link between TRYCAT and adaptive mechanisms involving mitochondrial respiration and synaptic plasticity might exist. This helps to better bring into context the essential networking of stress responsive systems during allostasis. The interconnectedness of the systems studied can be seen in Fig. 5. Importantly, allostatic processes in one system can influence the functioning of all other systems. This is beneficial if quick adaptations are vital, but conveys the risk of building up disturbances which cause instability of the network, transition of feedback loops from inhibitory regulation to promotion and subsequently switching to a pathological state (Stapelberg et al., 2018). Our findings on TRYCATs and IEGs substantiate the linking of the immune system with neuronal activity. Based on our respirometry findings, we propose the hypothesis of an energetic linkage between hippocampus and PFC which could help to explain further how disturbances in one system spread to the other and advance the likelihood to develop pathology. However, follow-up studies to verify this hypothesis are needed and some limitations should be considered when interpreting the presented results.

One limitation of our study is, that it was set up to investigate allostatic processes occurring early after onset of stress exposure, and so cannot make any firm conclusions as to eventual pathology. Testing the proposed suggestion that these allostatic mechanisms eventually fail and lead to pathology needs to be studies further. Profiling of the diurnal rhythm of corticosterone excretion indicated no changes in basal HPA-axis activity after 5 weeks of juvenile single-housing or after 5 additional weeks of uCMS exposure, suggesting that HPA-axis activity was not pathologically altered by the stress manipulation. However, no stress challenge was performed, since this could confound readouts from the other parameters accessed. Therefore, we cannot rule out that the responsiveness of the HPA-axis might have suffered during the stress manipulation. Importantly, appendix C indicates numerous correlations between different systems; ideally causal relationships should be demonstrated to support the interpretations. Dependent on the research question, amendment further improvement may be the use of brain parenchyma instead of CSF. By using CSF, we provide insights into a clinically applicable bio specimen, but studies aiming at elucidating mechanistically whether TRYCATs can effectively modulate plasticity via NMDA-receptor, tissue health, and mitochondrial function should detect catabolite levels within the tissue itself.

Currently 50–60 % of depressive patients do not respond to the first-line treatment (Fava and Davidson, 1996) and 30% do not reach remission even after several treatment attempts (Rush et al., 2006; Thase et al., 2007). Despite this unmet need for alternative treatments, no mechanistically new treatment options were reported lately and the

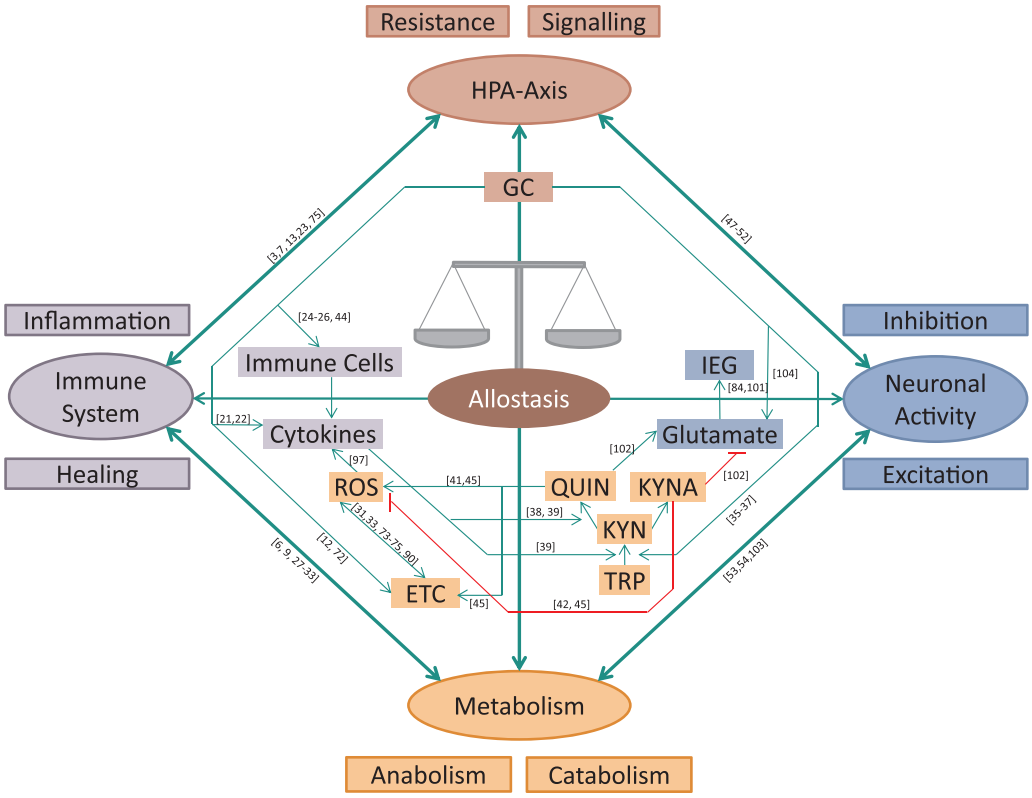

Fig. 5. Schematic of the Psycho-Immune-Neuro-Endocrine Network. Stress responsive systems interact with each other to adequately respond to stressors via allostatic processes. At the boarders, the HPA-axis (red), neuronal activity (blue), metabolism (orange) and the immune system (violet) are depicted as sentinel network nodes alongside with two extremes of their setting options. In the centre, the networking of representatives of these systems is visualized, while green arrows symbolize activation or feed-forward mechanisms and red arrows indicate inhibition. The numbers adjacent to the arrows represent selected publications included in the reference list which are further describing the link (For interpretation of the references to colour in this figure legend, the reader is referred to the web version of this article).

potential of classical approaches investigating the pathological state alone appeared to be exhausted. Hence, we selected the novel strategy to determine biomarkers pathology evidenced in patients in animals undergoing chronic stress. The potential to add stress-related 'prodromal' biomarkers can contribute to the mechanistic understanding of how pathology evolves. This could help to develop early diagnostic markers or even preventive treatment. In conclusion, this study demonstrated that allostatic processes allow the endurance of chronic exposure to mild stressors for a certain time and that juvenile single-housing stress has an influence on these processes. Both stress groups showed an increase in circulating immune cells, a decrease in the expression of immediate early genes in the PFC, and an increase in mitochondrial density in the hippocampus. However, only the double-hit of juvenile single housing stress and uCMS resulted in increased mitochondria respiration in the hippocampus. This increased metabolism might represent a cornerstone for later pathology, because increased mitochondrial activity goes hand in hand with increased ROS production, priming immune cells to pro-inflammatory actions (Naik and Dixit, 2011; Nakahira et al., 2011). This has extensively been described as starting point for functional disintegration of mitochondria (Yakes and Van Houten, 1997; Jendrach et al., 2008). From an evolutionary perspective, it is advantageous that adverse experiences during childhood and adolescence induce stress reactions are stronger and faster, to promote survival in inhospitable environments. However, this comes at the cost that individuals with adverse experiences during childhood or adolescence have an increased cumulative stress load. In a setting of chronic stress exposure, individuals with such a preconditioning may come closer to pathology and show signs of premature ageing than individuals without it. The increased mitochondrial respiration and amount of immune cells could be the beginning of the transition towards pathology, since these could lead over time to the development of oxidative stress and a pro-inflammatory milieu. To this end it would be interesting to know whether a longer duration of uCMS exposure would be sufficient to reach the tipping point, after which key physiological systems are out of balance and diseases develop. In such a longitudinal study, the transition from allostasis to pathology could be elucidated and a better timely resolution between the changes in energy metabolism and the immune system could help to understand the mechanistic linkage between both.

Declaration of interest

T. Bretschneider, N. Lawless, and KA Allers are employees of Boehringer Ingelheim Pharma GmbH KG.

Role of the funding source

The funding for this study was provided by Boehringer Ingelheim Pharma GmbH KG, to provide a master's thesis project to V. Nold. The company had no further influence on this work.

Submission declaration and verification

The hippocampal respirometry, blood counts and corticosterone measurements have been published in part as the Master's degree thesis of V. Nold, University of Ulm. The NGS analyses and TRYCAT measures as well as the statistical analyses were not part of the thesis.

CRediT authorship contribution statement

V. Nold: Conceptualization, Investigation, Writing - original draft, Formal analysis. **C. Sweatman:** Investigation, Conceptualization, Resources, Methodology. **A. Karabatsiakis:** Writing - review & editing, Investigation. **C. Böck:** Writing - review & editing, Investigation. **T. Bretschneider:** Resources, Methodology. **N. Lawless:** Resources, Formal analysis. **K. Fundel-Clemens:** Formal analysis, Resources. **I.-T. Kolassa:** Supervision, Writing - review & editing. **K.A. Allers:** Conceptualization, Project administration, Supervision, Writing - review & editing.

Acknowledgements

The authors would like to acknowledge Anna Lachenmaier and Anne-Kathrin Ludwig for their excellent assistance in the lab; Dr. med. Enrico Calzia and Prof. Dr. med. h. c Peter Radermacher for providing an additional high-resolution respirometer and guidance with the citrate synthase measurements; Dr. Tobias Hildebrandt for bioinformatics and NGS library preparation; and Dr. Stephan Kolassa and Dr. Moritz von Heimendal for their help with the statistics.

Appendix A. Supplementary data

Supplementary material related to this article can be found, in the online version, at doi:https://doi.org/10.1016/j.psyneuen.2019.04.006.

References

Anderson, M.C., Bunce, J.G., Barbas, H., 2016. Prefrontal-hippocampal pathways underlying inhibitory control over memory. Neurobiol. Learn. Mem. 134 (Pt A(Pt A)), 145–161.
Armario, A., Gavalda, A., Marti, J., 1995. Comparison of the behavioural and endocrine response to forced swimming stress in five inbred strains of rats. Psychoneuroendocrinology 20 (8), 879–890.
Asp, L., et al., 2011. Effects of pro-inflammatory cytokines on expression of kynurenine pathway enzymes in human dermal fibroblasts. J. Inflamm. (Lond) 8, 25.
Assmann, N., Finlay, D.K., 2016. Metabolic regulation of immune responses: therapeutic opportunities. J. Clin. Invest. 126 (6), 2031–2039.
Bauer, M.E., 2008. Chronic stress and immunosenescence: a review. Neuroimmunomodulation 15 (4-6), 241–250.
Baum, A.E., et al., 2006. Test- and behavior-specific genetic factors affect WKY hypoactivity in tests of emotionality. Behav. Brain Res. 169 (2), 220–230.
Becker, J.B., Prendergast, B.J., Liang, J.W., 2016. Female rats are not more variable than male rats: a meta-analysis of neuroscience studies. Biol. Sex Differ. 7, 34.
Belleau, E.L., Treadway, M.T., Pizzagalli, D.A., 2018. The impact of stress and major depressive disorder on hippocampal and medial prefrontal cortex morphology. Biol. Psychiatry.
Bisht, K., Sharma, K., Tremblay, M.E., 2018. Chronic stress as a risk factor for Alzheimer's disease: roles of microglia-mediated synaptic remodeling, inflammation, and oxidative stress. Neurobiol. Stress 9, 9–21.
Boeck, C., et al., 2018. Targeting the association between telomere length and immunocellular bioenergetics in female patients with Major Depressive Disorder. Sci. Rep. 8 (1), 9419.
Buttgereit, F., Burmester, G.R., Brand, M.D., 2000. Bioenergetics of immune functions: fundamental and therapeutic aspects. Immunol. Today 21 (4), 192–199.
Campbell, B.M., et al., 2014. Kynurenines in CNS disease: regulation by inflammatory cytokines. Front. Neurosci. 8, 12.
Capuron, L., Miller, A.H., 2011. Immune system to brain signaling: neuropsychopharmacological implications. Pharmacol. Ther. 130 (2), 226–238.
Chen, W.L., et al., 2018a. The impact of occupational psychological hazards and metabolic syndrome on the 8-year risk of cardiovascular diseases-A longitudinal study. PLoS One 13 (8), e0202977.
Chen, Y., Zhou, Z., Min, W., 2018b. Mitochondria, oxidative stress and innate immunity. Front. Physiol. 9, 1487.
De, R., et al., 2017. Acute mental stress induces mitochondrial bioenergetic crisis and hyper-fission along with aberrant mitophagy in the gut mucosa in rodent model of stress-related mucosal disease. Free Radic. Biol. Med. 113, 424–438.
De Pitta, M., Brunel, N., 2016. Modulation of synaptic plasticity by glutamatergic gliotransmission: a modeling study. Neural Plast. 2016, 7607924.
de Punder, K., et al., 2018. Inflammatory measures in depressed patients with and without a history of adverse childhood experiences. Front. Psychiatry 9, 610.
Deak, T., et al., 2017. A multispecies approach for understanding neuroimmune mechanisms of stress. Dialogues Clin. Neurosci. 19 (1), 37–53.
Delmastro-Greenwood, M.M., Piganelli, J.D., 2013. Changing the energy of an immune response. Am. J. Clin. Exp. Immunol. 2 (1), 30–54.
Demir, S., et al., 2015. Neutrophil-lymphocyte ratio in patients with major depressive disorder undergoing no pharmacological therapy. Neuropsychiatr. Dis. Treat. 11, 2253–2258.
Demirtas, T., et al., 2014. The link between unpredictable chronic mild stress model for depression and vascular inflammation? Inflammation 37 (5), 1432–1438.
Deschenes, S.S., et al., 2018. Adverse childhood experiences and the risk of diabetes: examining the roles of depressive symptoms and cardiometabolic dysregulations in the whitehall II cohort study. Diabetes Care 41 (10), 2120–2126.
Dhabhar, F.S., et al., 2012. Stress-induced redistribution of immune cells—from barracks to boulevards to battlefields: a tale of three hormones—curt Richter Award winner. Psychoneuroendocrinology 37 (9), 1345–1368.
Doolin, K., et al., 2018. Altered tryptophan catabolite concentrations in major depressive disorder and associated changes in hippocampal subfield volumes. Psychoneuroendocrinology 95, 8–17.
Entringer, S., Buss, C., Heim, C., 2016. Early-life stress and vulnerability for disease in later life. Bundesgesundheitsblatt Gesundheitsforschung Gesundheitsschutz 59 (10), 1255–1261.
Eo, W.K., et al., 2016. The lymphocyte-monocyte ratio predicts patient survival and aggressiveness of endometrial cancer. J. Cancer 7 (5), 538–545.
Fava, M., Davidson, K.G., 1996. Definition and epidemiology of treatment-resistant depression. Psychiatr. Clin. North Am. 19 (2), 179–200.
Foyet, H.S., et al., 2017. Ficus sycomorus extract reversed behavioral impairment and brain oxidative stress induced by unpredictable chronic mild stress in rats. BMC Complement. Altern. Med. 17 (1), 502.
Fukui, S., et al., 1991. Blood-brain barrier transport of kynurenines: implications for brain synthesis and metabolism. J. Neurochem. 56 (6), 2007–2017.
Gibney, S.M., et al., 2014. Inhibition of stress-induced hepatic tryptophan 2,3-dioxygenase exhibits antidepressant activity in an animal model of depressive behaviour. Int. J. Neuropsychopharmacol. 17 (6), 917–928.
Godsil, B.P., et al., 2013. The hippocampal-prefrontal pathway: the weak link in psychiatric disorders? Eur. Neuropsychopharmacol. 23 (10), 1165–1181.
Goldwater, D.S., et al., 2009. Structural and functional alterations to rat medial prefrontal cortex following chronic restraint stress and recovery. Neuroscience 164 (2), 798–808.
Gomes, F.V., Rincon-Cortes, M., Grace, A.A., 2016. Adolescence as a period of vulnerability and intervention in schizophrenia: insights from the MAM model. Neurosci. Biobehav. Rev. 70, 260–270.
Gomez, F., et al., 1996. Hypothalamic-pituitary-adrenal response to chronic stress in five inbred rat strains: differential responses are mainly located at the adrenocortical level. Neuroendocrinology 63 (4), 327–337.
Han, M.H., Nestler, E.J., 2017. Neural substrates of depression and resilience. Neurotherapeutics 14 (3), 677–686.
Holmes, S.E., et al., 2018. Cerebellar and prefrontal cortical alterations in PTSD: structural and functional evidence. Chronic Stress (Thousand Oaks) 2.
Hunt, D.L., Castillo, P.E., 2012. Synaptic plasticity of NMDA receptors: mechanisms and functional implications. Curr. Opin. Neurobiol. 22 (3), 496–508.
Indo, H.P., et al., 2007. Evidence of ROS generation by mitochondria in cells with impaired electron transport chain and mitochondrial DNA damage. Mitochondrion 7 (1-2), 106–118.
Jay, T.M., 2003. Dopamine: a potential substrate for synaptic plasticity and memory mechanisms. Prog. Neurobiol. 69 (6), 375–390.
Jendrach, M., et al., 2008. Short- and long-term alterations of mitochondrial morphology, dynamics and mtDNA after transient oxidative stress. Mitochondrion 8 (4), 293–304.
Karabatsiakis, A., Böck, C., Salinas-Manrique, J., Kolassa, S., Calzia, E., Dietrich, D.E., Kolassa, I.T., 2014. Mitochondrial respiration in peripheral blood mononuclear cells correlates with depressive subsymptoms and severity of major depression. Transl Psychiatry 10 (4), e397. https://doi.org/10.1038/tp.2014.44.
Kitaoka, S., Furuyashiki, T., 2014. Roles of inflammation-related molecules in emotional changes induced by repeated stress. Nihon Shinkei Seishin Yakurigaku Zasshi 34 (4), 109–115.
Kraynak, T.E., et al., 2018. Functional neuroanatomy of peripheral inflammatory physiology: a meta-analysis of human neuroimaging studies. Neurosci. Biobehav. Rev. 94, 76–92.
Larsen, S., et al., 2012. Biomarkers of mitochondrial content in skeletal muscle of healthy young human subjects. J. Physiol. 590 (14), 3349–3360.
Liu, Y., Fiskum, G., Schubert, D., 2002. Generation of reactive oxygen species by the mitochondrial electron transport chain. J. Neurochem. 80 (5), 780–787.
Lopez-Armada, M.J., et al., 2013. Mitochondrial dysfunction and the inflammatory response. Mitochondrion 13 (2), 106–118.
Lugo-Huitron, R., et al., 2011. On the antioxidant properties of kynurenic acid: free radical scavenging activity and inhibition of oxidative stress. Neurotoxicol. Teratol. 33 (5), 538–547.
Maes, M., et al., 2012. New drug targets in depression: inflammatory, cell-mediated immune, oxidative and nitrosative stress, mitochondrial, antioxidant, and neuroprogressive pathways. And new drug candidates—Nrf2 activators and GSK-3 inhibitors. Inflammopharmacology 20 (3), 127–150.
Mattson, M.P., 2008. Glutamate and neurotrophic factors in neuronal plasticity and disease. Ann. N. Y. Acad. Sci. 1144, 97–112.
McEwen, B.S., 2004. Protection and damage from acute and chronic stress: allostasis and allostatic overload and relevance to the pathophysiology of psychiatric disorders. Ann. N. Y. Acad. Sci. 1032, 1–7.
Mellon, S.H., et al., 2018. Metabolism, metabolomics, and inflammation in posttraumatic stress disorder. Biol. Psychiatry 83 (10), 866–875.
Miller, G.E., Cohen, S., Ritchey, A.K., 2002. Chronic psychological stress and the regulation of pro-inflammatory cytokines: a glucocorticoid-resistance model. Health Psychol. 21 (6), 531–541.
Minatohara, K., Akiyoshi, M., Okuno, H., 2015. Role of immediate-early genes in synaptic plasticity and neuronal ensembles underlying the memory trace. Front. Mol. Neurosci. 8, 78.
Mo, Y., et al., 2014. Alteration of behavioral changes and hippocampus galanin expression in chronic unpredictable mild stress-induced depression rats and effect of electroacupuncture treatment. Evid. Complement. Alternat. Med. 2014, 179796.
Naik, E., Dixit, V.M., 2011. Mitochondrial reactive oxygen species drive proinflammatory cytokine production. J. Exp. Med. 208 (3), 417–420.
Nakahira, K., et al., 2011. Autophagy proteins regulate innate immune responses by inhibiting the release of mitochondrial DNA mediated by the NALP3 inflammasome. Nat. Immunol. 12 (3), 222–230.
Nikolaienko, O., et al., 2018. Arc protein: a flexible hub for synaptic plasticity and cognition. Semin. Cell Dev. Biol. 77, 33–42.
Notarangelo, F.M., Pocivavsek, A., Schwarcz, R., 2018. Exercise your kynurenines to fight depression. Trends Neurosci. 41 (8), 491–493.

Ohno, I., 2017. Neuropsychiatry phenotype in asthma: psychological stress-induced alterations of the neuroendocrine-immune system in allergic airway inflammation. Allergol. Int. 66s, S2–s8.
Ohta, Y., et al., 2017. Effect of water-immersion restraint stress on tryptophan catabolism through the kynurenine pathway in rat tissues. J. Physiol. Sci. 67 (3), 361–372.
Opel, N., et al., 2014. Hippocampal atrophy in major depression: a function of childhood maltreatment rather than diagnosis? Neuropsychopharmacology 39 (12), 2723–2731.
Osborne, D.M., Pearson-Leary, J., McNay, E.C., 2015. The neuroenergetics of stress hormones in the hippocampus and implications for memory. Front. Neurosci. 9, 164.
Otani, S., et al., 2003. Dopaminergic modulation of long-term synaptic plasticity in rat prefrontal neurons. Cereb. Cortex 13 (11), 1251–1256.
Patist, C.M., et al., 2018. The brain-adipocyte-gut network: linking obesity and depression subtypes. Cogn. Affect. Behav. Neurosci. 18 (6), 1121–1144.
Pearce, E.L., Pearce, E.J., 2013. Metabolic pathways in immune cell activation and quiescence. Immunity 38 (4), 633–643.
Pearson-Leary, J., et al., 2017. Inflammation and vascular remodeling in the ventral hippocampus contributes to vulnerability to stress. Transl. Psychiatry 7 (6), e1160.
Pérez-De La Cruz, V., Carrillo-Mora, P., Santamaría, A., 2012. Quinolinic acid, an endogenous molecule combining excitotoxicity, oxidative stress and other toxic mechanisms. Int. J. Tryptophan Res. 5, 1–8.
Pesta, D., Gnaiger, E., 2012. High-resolution respirometry: OXPHOS protocols for human cells and permeabilized fibers from small biopsies of human muscle. Methods Mol. Biol. 810, 25–58.
Piskunov, A., et al., 2016. Chronic combined stress induces selective and long-lasting inflammatory response evoked by changes in corticosterone accumulation and signaling in rat hippocampus. Metab. Brain Dis. 31 (2), 445–454.
Popoli, M., et al., 2011. The stressed synapse: the impact of stress and glucocorticoids on glutamate transmission. Nat. Rev. Neurosci. 13 (1), 22–37.
PS216, 2016. Preclinical and clinical assessment of tryptophan catabolites (TRYCATS) as a measure of neuroinflammation and utility in compound screening. Int. J. Neuropsychopharmacol. 27;19 (May Suppl 1), 79. https://doi.org/10.1093/ijnp/pyw043.216. eCollection 2016 Jun.
Rebola, N., Srikumar, B.N., Mulle, C., 2010. Activity-dependent synaptic plasticity of NMDA receptors. J. Physiol. 588 (Pt 1), 93–99.
Redei, E.E., et al., 2001. Paradoxical hormonal and behavioral responses to hypothyroid and hyperthyroid states in the Wistar-Kyoto rat. Neuropsychopharmacology 24 (6), 632–639.
Rezin, G.T., et al., 2008. Inhibition of mitochondrial respiratory chain in brain of rats subjected to an experimental model of depression. Neurochem. Int. 53 (6-8), 395–400.
Rupprecht, A., et al., 2012. Quantification of uncoupling protein 2 reveals its main expression in immune cells and selective up-regulation during T-cell proliferation. PLoS One 7 (8), e41406.
Rush, A.J., et al., 2006. Acute and longer-term outcomes in depressed outpatients requiring one or several treatment steps: a STAR*D report. Am. J. Psychiatry 163 (11), 1905–1917.
Sahin, T.D., et al., 2017. Penile constitutive nitric oxide synthase expression in rats exposed to unpredictable chronic mild stress: role of inflammation. Int. J. Impot. Res. 29 (2), 76–81.
Sas, K., et al., 2007. Mitochondria, metabolic disturbances, oxidative stress and the kynurenine system, with focus on neurodegenerative disorders. J. Neurol. Sci. 257 (1-2), 221–239.
Schwarcz, R., 2016. Kynurenines and Glutamate: Multiple Links and Therapeutic Implications. Adv. Pharmacol. 76, 13–37.
Sheline, Y.I., et al., 1996. Hippocampal atrophy in recurrent major depression. Proc. Natl. Acad. Sci. U. S. A. 93 (9), 3908–3913.
Shepard, R., Coutellier, L., 2018. Changes in the prefrontal glutamatergic and parvalbumin systems of mice exposed to unpredictable chronic stress. Mol. Neurobiol. 55 (3), 2591–2602.
Smith, M.A., 1996. Hippocampal vulnerability to stress and aging: possible role of neurotrophic factors. Behav. Brain Res. 78 (1), 25–36.
Smith, D.G., et al., 2001. Quinolinic acid is produced by macrophages stimulated by platelet activating factor. Nef. Tat. J. Neurovirol. 7 (1), 56–60.
Soichot, M., et al., 2013. Characterization of functional polymorphisms and glucocorticoid-responsive elements in the promoter of TDO2, a candidate gene for ethanol-induced behavioural disorders. Alcohol Alcohol. 48 (4), 415–425.
Solberg, L.C., et al., 2001. Altered hormone levels and circadian rhythm of activity in the WKY rat, a putative animal model of depression. Am. J. Physiol. Regul. Integr. Comp. Physiol. 281 (3), R786–94.
Sollner, J.F., et al., 2017. An RNA-Seq atlas of gene expression in mouse and rat normal tissues. Sci. Data 4, 170185.
Srivastava, R., et al., 2018. Dynamic changes of the mitochondria in psychiatric illnesses: new mechanistic insights from human neuronal models. Biol. Psychiatry 83 (9), 751–760.
Stapelberg, N.J.C., et al., 2018. From feedback loop transitions to biomarkers in the psycho-immune-neuroendocrine network: detecting the critical transition from health to major depression. Neurosci. Biobehav. Rev. 90, 1–15.
Stefanaki, C., et al., 2018. Chronic stress and body composition disorders: implications for health and disease. Hormones (Athens) 17 (1), 33–43.
Stotz, M., et al., 2015. The lymphocyte to monocyte ratio in peripheral blood represents a novel prognostic marker in patients with pancreatic cancer. Clin. Chem. Lab. Med. 53 (3), 499–506.
Swan, M.P., Hickman, D.L., 2014. Evaluation of the neutrophil-lymphocyte ratio as a measure of distress in rats. Lab Anim. (NY) 43 (8), 276–282.
Takahashi, A., Miczek, K.A., 2014. Neurogenetics of aggressive behavior: studies in rodents. Curr. Top. Behav. Neurosci. 17, 3–44.
Takaki, M., et al., 1997. No suppression of respiratory function of mitochondrial isolated from the hearts of anesthetized rats with high-dose pentobarbital sodium. Jpn. J. Physiol. 47 (1), 87–92.
Thase, M.E., et al., 2007. Efficacy of duloxetine and selective serotonin reuptake inhibitors: comparisons as assessed by remission rates in patients with major depressive disorder. J. Clin. Psychopharmacol. 27 (6), 672–676.
Tynan, R.J., et al., 2010. Chronic stress alters the density and morphology of microglia in a subset of stress-responsive brain regions. Brain Behav. Immun. 24 (7), 1058–1068.
Tzanoulinou, S., Sandi, C., 2017. The programming of the social brain by stress during childhood and adolescence: from rodents to humans. Curr. Top. Behav. Neurosci. 30, 411–429.
Wang, M., et al., 2014. Synaptic modifications in the medial prefrontal cortex in susceptibility and resilience to stress. J. Neurosci. 34 (22), 7485–7492.
Wang, J., et al., 2015. Ratio of monocytes to lymphocytes in peripheral blood in patients diagnosed with active tuberculosis. Braz. J. Infect. Dis. 19 (2), 125–131.
Will, C.C., Aird, F., Redei, E.E., 2003. Selectively bred Wistar-Kyoto rats: an animal model of depression and hyper-responsiveness to antidepressants. Mol. Psychiatry 8 (11), 925–932.
Wirtz, P.H., von Kanel, R., 2017. Psychological stress, inflammation, and coronary heart disease. Curr. Cardiol. Rep. 19 (11), 111.
Wright, R.J., 2009. Stress and acquired glucocorticoid resistance: a relationship hanging in the balance. J. Allergy Clin. Immunol. 123 (4), 831–832.
Yakes, F.M., Van Houten, B., 1997. Mitochondrial DNA damage is more extensive and persists longer than nuclear DNA damage in human cells following oxidative stress. Proc. Natl. Acad. Sci. U. S. A. 94 (2), 514–519.
Zannas, A.S., Binder, E.B., 2014. Gene-environment interactions at the FKBP5 locus: sensitive periods, mechanisms and pleiotropism. Genes Brain Behav. 13 (1), 25–37.